

Source characterization of induced earthquakes by the 2011 off Tohoku, Japan, earthquake based on the strong motion simulations

K. Somei & K. Miyakoshi

Geo-Reserch Institute, Osaka, Japan



SUMMARY:

A great inter-plate earthquake (M_w 9.0) occurred at the off Tohoku, Japan, on March 11, 2011 (JST). In addition to the inter-plate aftershocks, some of large ‘induced earthquakes’ have generated extreme large ground motions. For understanding source characteristics of these induced earthquakes, we focus on the source parameter scaling with empirical relationships. From the forward strong motion simulations based on the empirical Green's function method, the characterized source models composed by strong motion generation areas (SMGA) of three induced earthquakes were estimated. Three induced earthquakes are the 2011 Shizuoka-ken Toubu earthquake, the 2011 Miyagi-ken oki intra-slab earthquake, and the 2011 Fukushima-ken Hamadori earthquake. We found that the SMGA parameters of these events (two inland crustal events and one intra-slab event) follow the empirical scaling relationships of previous studies for each tectonic environment, i.e. for inland crustal earthquakes (e.g. Somerville *et al.*, 1999), for intra-slab earthquake (e.g. Iwata and Asano, 2011).

Keywords: 2011 off Tohoku, Japan, earthquake, Induced earthquake, source model

1. INTRODUCTION

On March 11, 2011 (JST), a great inter-plate earthquake (M_w 9.0) occurred at the off Pacific coast of Tohoku, Japan with severe damages related to ground motion and tsunami (hereafter we call this earthquake ‘2011 Tohoku earthquake’). To reveal the detailed source rupture process and the mechanism of strong motion generation during the 2011 Tohoku earthquake, several studies have constructed the source models from various observed records (e.g., Yoshida *et al.*, 2011; Koketsu *et al.*, 2011; Kurahashi and Irikura, 2011).

In addition to the inter-plate aftershocks, seismic activities have significantly increased in almost the entire area of the northeast Japan after the 2011 Tohoku earthquake (e.g., Okada *et al.*, 2011; Toda *et al.*, 2011), and many large earthquakes greater than M_w 5.0 have also occurred in non-inter-plate conditions (Figure 1). In this paper, we call these non-inter-plate large aftershocks ‘induced earthquakes’. The seismic moments of these earthquakes are relative smaller than that of 2011 Tohoku earthquake (M_w 9.0), while the large ground motion were also observed by some of induced earthquakes (e.g., the 2011 Shizuoka-ken Toubu inland crustal earthquake; the 2011 Miyagi-ken oki intra-slab earthquake; the 2011 Fukushima-ken Hamadori earthquake). The 2011 Fukushima-ken Hamadori earthquake is a shallow inland crustal earthquake with normal fault-type mechanism which is rarity in Japan. This normal fault-type event may have activated by a tensional stress change caused by the mega-thrust faulting of the 2011 Tohoku earthquake (Asano *et al.*, 2011).

It is also important to focus on the source models and strong motion generations during these large induced earthquakes, not only those of 2011 Tohoku earthquake. We start to collect source models of induced earthquakes with a same procedure which is the forward modeling through strong motion simulations using the empirical Green's function method (e.g., Irikura, 1986; Kamae and Irikura, 1988; Miyake *et al.*, 2003). Next we compare the source parameters based on the characterized source model

with the previous studies and empirical relationship.

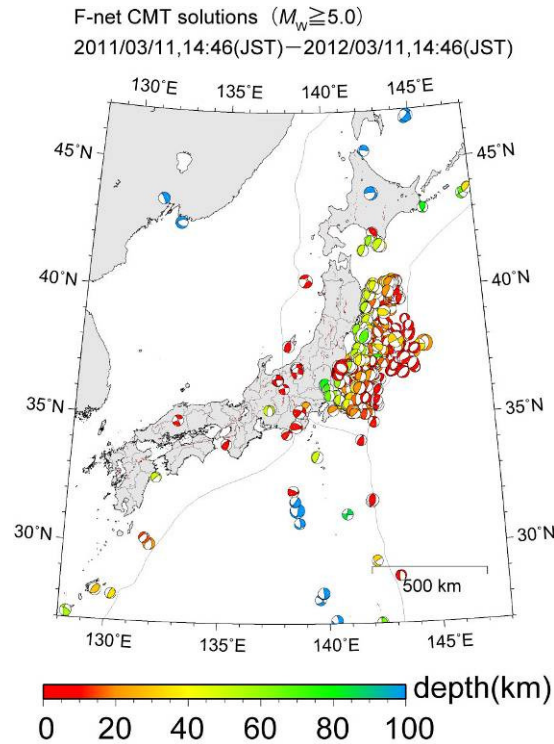


Figure 1. Spatial distribution of earthquakes greater than M_w 5.0 within 1 year after the 2011 Tohoku earthquake with focal mechanisms from F-net (Fukuyama *et al.*, 2003) catalogue which is operated by National Research Institute for Earth Science and Disaster Prevention Japan (NIED).

2. STRONG MOTION DATA AND METHOD

For this study, we selected source models of three induced earthquakes obtained by the strong motion fitting. The three earthquakes are the 2011 Shizuoka-ken Toubu inland crustal earthquake, the 2011 Miyagi-ken oki intra-slab earthquake, and the 2011 Fukushima-ken Hamadori inland crustal earthquake. Figure 2 shows the epicenters and source mechanisms of the three earthquakes. The hypocentral information for these events is listed in Table 1. The source models of these events are obtained by the forward simulation over a wide frequency range based on the empirical Green's function (EGF) method (Irikura, 1986). In the following sections, we briefly explain the processes of constructing source models according to Somei *et al.* (2011, 2012a, 2012b).

2.1. Features of the observed strong motions

The ground motions from each induced earthquake sequence were densely observed by the nation wide strong motion seismograph networks, K-NET (Kinoshita, 1998) and KiK-net (Aoi *et al.*, 2000), installed by NIED, and the Onagawa nuclear power plant by Tohoku Electric Power Company. For the events No.1 and No.2, several strong motion stations especially near the sources have recorded extremely large ground motions with peak ground acceleration (PGA) greater than 1000cm/s^2 . These observed values are larger than the empirical relationships proposed by Si and Midorikawa (1999), while the observed PGA values at other sites are comparable to the empirical relationship through the whole distances for each events (Figure 3). In order to understand the physical mechanism of the ground-motion generation process during these earthquakes, a reliable source models needs to be constructed.

2.2. Empirical Green's function method

The EGF method is a technique used to synthesize seismic records by summing up the observed records of small earthquakes as empirical Green's functions. Hereafter we call these small earthquakes 'element earthquakes'. By this method we can therefore simulate realistic waveforms up to high frequencies that are affected by minute heterogeneous propagation-path structures. The characters "m" and "a" in the first column in Table 1 indicate mainshock and element earthquake, respectively. As stated previously, we defined the strong motion generation area (SMGA) as the area characterized by a large uniform slip velocity within total rupture area, which reproduces near source strong motions up to 10 Hz. The parameters of SMGA of each event are estimated by waveform fitting between the observed seismic records and the synthesized seismic records.

Table 1. List of earthquake studied in this paper

No.	Org.time (JST) ^{*1} (y/m/d,h,m,s)	Latitude ^{*1} (deg.)	Longitude ^{*1} (deg.)	Depth ^{*1} (km)	M_{JMA} ^{*1}	M_0 ^{*2} (Nm)	M_w ^{*2}	Name of earthquake (TC ^{*4}) / Reference
1m	2011/03/15,22:31:46.34	35.3095N	138.7145E	14.31	6.4	8.38×10^{17}	5.9	2011 Shizuoka-ken Toubu (IC)
1a	2011/03/15,22:40:36.72	35.3070N	138.7030E	14.00	4.2	3.72×10^{15} ^{*3}	4.3 ^{*3}	/ Somei <i>et al.</i> (2012a)
2m	2011/04/07,23:32:43.46	38.2028N	141.9237E	65.90	7.2	4.74×10^{19}	7.1	2011 Miyagi-ken Oki (IS)
2a	2011/07/13,00:37:23.24	38.3312N	142.0072E	47.20	4.9	2.64×10^{16}	4.9	/ Somei <i>et al.</i> (2012b)
3m	2011/04/11,17:16:12.02	36.9457N	140.6727E	6.42	7.0	9.58×10^{18}	6.6	2011 Fukushima-ken Hamadori (IC)
3a	2011/05/03,22:57:14.86	37.0130N	140.5853E	8.46	4.5	2.75×10^{15}	4.2	/ Somei <i>et al.</i> (2011)

*1: Hypocenter information from Japan Meteorological Agency (JMA)

*2: Moment tensor solution of F-net operated by the National Research Institute for Earth Science and Disaster Prevention Japan (NIED)

*3: Seismic moment determined by Somei *et al.* (2012a)

*4: Tectonic condition (IC: Inland crustal earthquake, IS: Intra-slab earthquake)

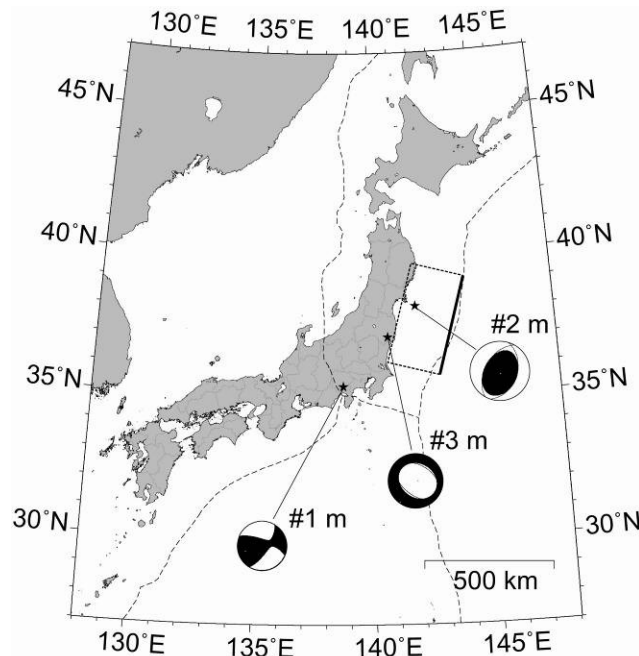


Figure 2. Epicenter locations (stars) and focal mechanism obtained by F-net of the earthquakes studied in this paper. The dotted rectangle denotes the assumed fault plane of the 2011 Tohoku earthquake by Yoshida *et al.* (2011).

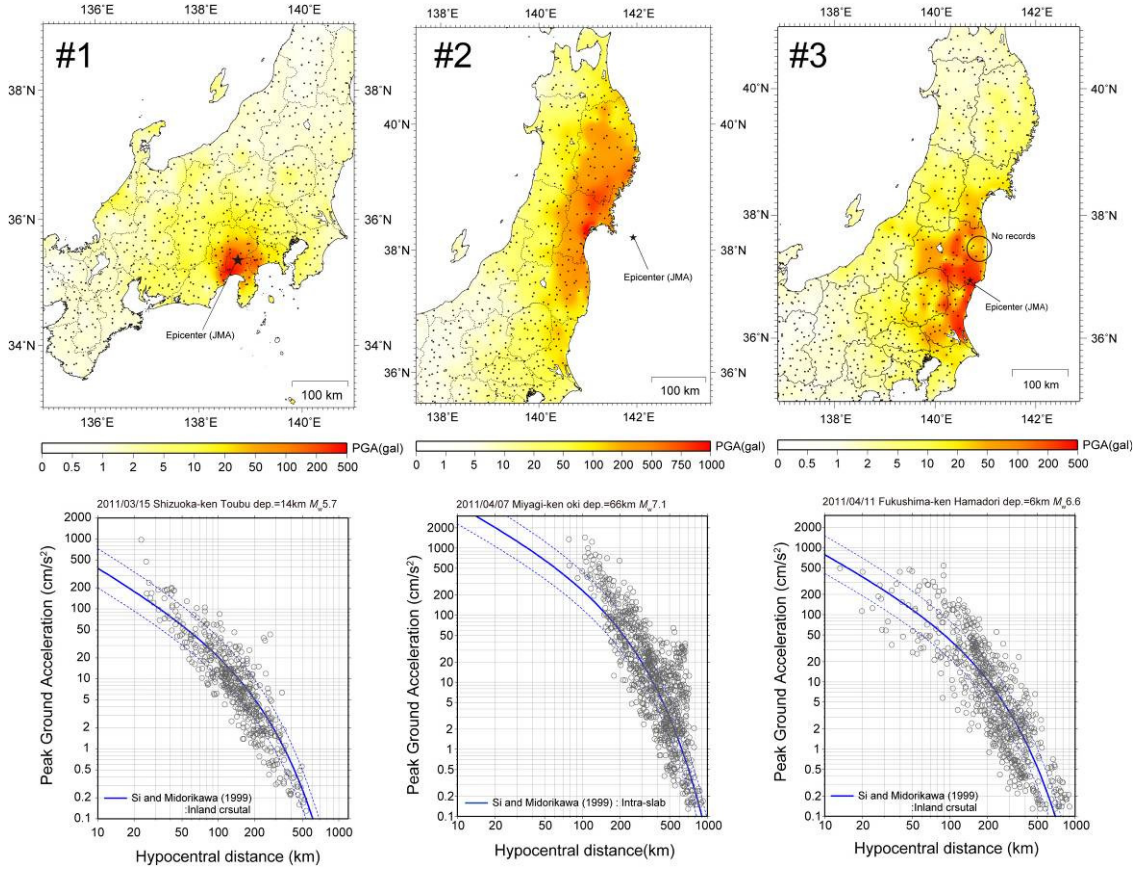


Figure 3. Top: Spatial distribution of peak ground acceleration (PGA) from each induced earthquake. The star is the epicenter of each event. Black dots indicate K-NET and KiK-net stations. Bottom: Distribution of PGA values over distance. The empirical relationship (solid curve) and standard deviations (dashed curves) proposed by Si and Midorikawa (1999) are also shown.

In terms of constructing source models, strong motion records observed at 20 stations of K-NET, KiK-net and the Onagawa site surrounding source area are used for each event (Figure 4). For the KiK-net and Onagawa stations, downhole sensor records are used. We first estimate source characteristics, i.e. corner frequency and rupture area, of the element earthquakes by comparing the observed source spectra with ω^{-2} source spectral model (Brune, 1970, 1971). Based on the rupture area of element earthquakes, we next estimate the source models of each induced earthquake by minimizing the misfit between observed waveforms and synthesized waveforms. Synthesized waveforms are simulated by using the EGF method. First, we employ the grid-search for estimating the source model in order to evaluate broadband waveforms by minimizing the following misfit function (Suzuki and Iwata, 2005, 2006).

$$\text{misfit} = \frac{\int (u_{\text{obs}} - u_{\text{syn}})^2 dt}{\sqrt{\int u_{\text{obs}}^2 dt} \sqrt{\int u_{\text{syn}}^2 dt}} + \frac{\int (e_{\text{obs}} - e_{\text{syn}})^2 dt}{\sqrt{\int e_{\text{obs}}^2 dt} \sqrt{\int e_{\text{syn}}^2 dt}} \quad (2.1)$$

Here, u is the velocity waveform, while e is the envelope of the acceleration waveform. Both velocity and acceleration waveforms are bandpass-filtered between 0.2 (or 0.3) – 10 Hz. The lower frequency limit is determined from the Signal/Noise ratio of element earthquakes. We finally estimate the best fit source model through a trial and error process by comparing observed waveforms with synthesized waveforms of acceleration, velocity, and displacement. We assumed rectangular SMGAs, and the SMGA1 is assumed to include the hypocenter determined by Japan Meteorological Agency (JMA). The estimated model parameters are the rupture starting subfault of each SMGA, rise time, rupture velocity, and the location of the SMGA2 or SMGA3.

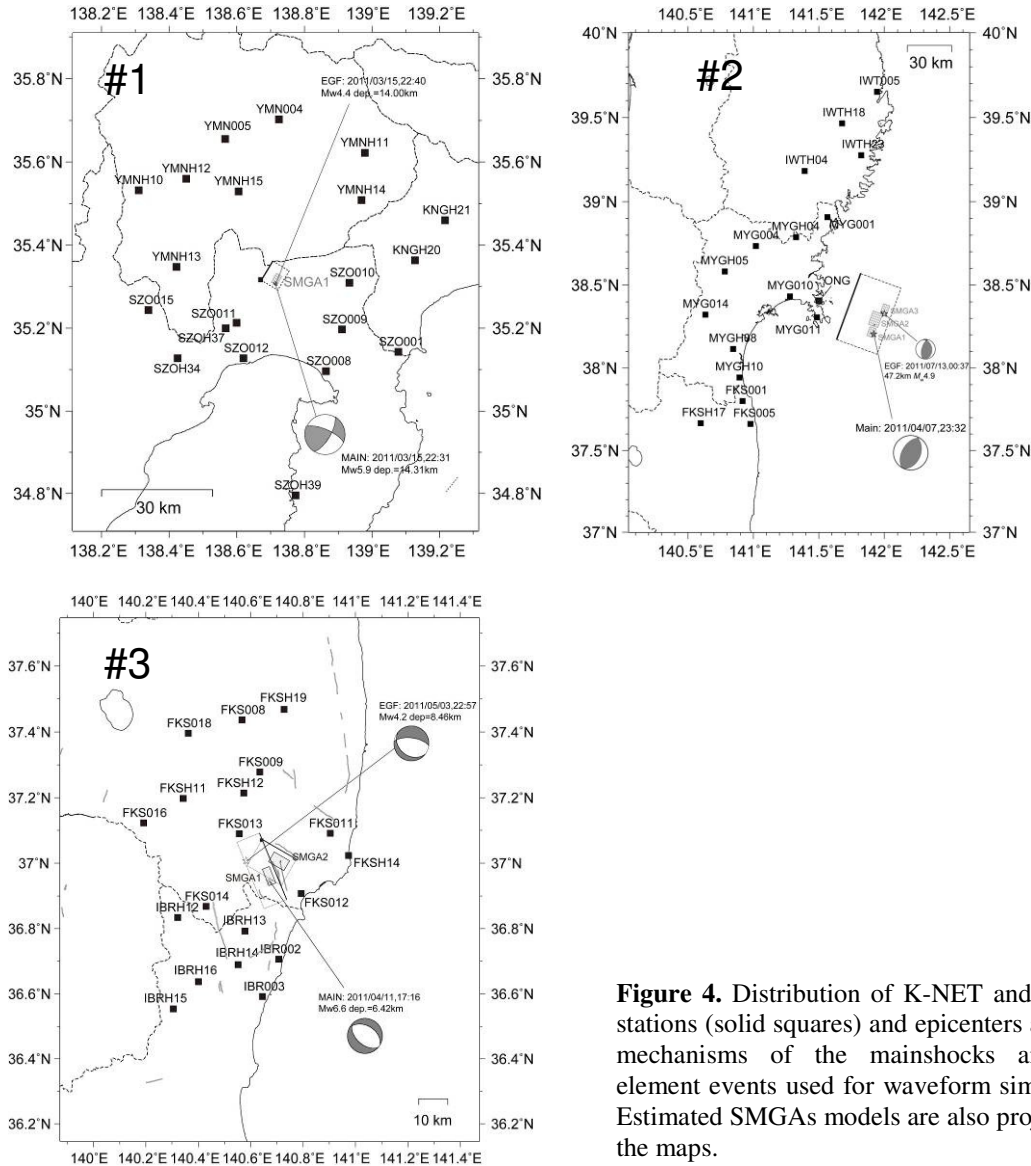


Figure 4. Distribution of K-NET and KiK-net stations (solid squares) and epicenters and focal mechanisms of the mainshocks and EGF element events used for waveform simulations. Estimated SMGAs models are also projected on the maps.

3. SOURCE MODELS AND STRONG MOTION SIMULATIONS

The obtained SMGA models on the faults are shown in Figure 5, and also projected on maps in Figure 4. Using the parameters listed in Table 2, we perform strong motion simulations of induced earthquakes. Synthetic velocity waveforms for the best source models explain the observed records fairly well (Figure 6).

Event No.1 (the 2011 Shizuoka-ken Toubu earthquake) is an inland crustal earthquake occurred nearly beneath the Mt. Fuji, and recorded extreme ground motion at SZO011 station (Figure 4, 6). This earthquake has a single SMGA which rupture mainly propagates upward along the dip direction. Meanwhile, there are no extreme source characteristics, i.e. the high stress drop in SMGA, to bring the large ground motion to SZO011. However, the synthetic waveform from the best source model duplicates the observed waveform at the SZO011. On the other, the ground motion records at SZO011 from the other earthquakes tend to have relative larger amplitude than that of SZOH37 which is a rock site close to SZO011. Therefore, the extreme large ground motion at SZO011 during the event #1 is mainly caused by site amplification and upward directivity effect along fault dip direction (Somei *et al.*, 2012a).

Event No.2 (the 2011 Miyagi-ken oki earthquake) is an intra-slab earthquake occurred within the subducting Pacific plate beneath off Miyagi prefecture. We found that in order to explain the observed strong motion records, this earthquake should be composed of three SMGAs, which have different rupture directivities. The stress drop of each SMGA is estimated to be 23.7MPa, 70.8MPa, 70.8MPa. The rupture of SMGA1 including the hypocenter of mainshock mainly propagates westward, and that of SMGA2 mainly propagates northwestward. These SMGAs are ruptured propagating forward Tohoku region, Japan. The each forward directivity effect by SMGA1 and SMGA2 contribute to the pulse waveforms observed at MYG011 located in Ojika peninsula and the stations located in South coast of Iwate prefecture respectively. While, the rupture of SMGA3 propagates eastward that is back away from Tohoku region. This backward directivity effect by SMGA3 generates the relative long lapse time waveforms (Somei *et al.*, 2012b).

Event No.3 (the Fukushima-ken Hamadori earthquake) is an inland crustal earthquake. After this earthquake, distinct normal fault type surface ruptures were recognized during field survey in the source area (Ishiyama *et al.*, 2011). Surface ruptures line up along the two previously-known fault traces (Idosawa segment and Yunodake segment). Additionally, two S-wave packets are clearly observed in the records at strong motion stations where located around the source area. The first S-wave velocity pulse is sharply observed at the stations located to north of the hypocenter especially. The obtained source model of this event has one SMGA for each segment. The stress drops of both SMGAs are estimated to be 14.6MPa. The rupture process of SMGA1 mainly propagates northward from the hypocenter, and this rupture directivity contributes to generate the first S-wave velocity pulse (Somei *et al.*, 2011).

Table 2. Estimated parameters of SMGAs from EGF simulations

	#1	#2			#3	
	SMGA1	SMGA1	SMGA2	SMGA3	SMGA1	SMGA2
Area (km ²)	26.6	35.6	80.1	35.6	39.5	39.5
Rise time (s)	0.40	0.60	0.60	0.60	0.60	0.60
M_0 (Nm)	9.5×10^{17}	2.1×10^{18}	2.1×10^{19}	6.2×10^{18}	1.5×10^{18}	1.5×10^{18}
Stress drop (MPa)	16.9	23.7	70.8	70.8	14.6	14.6
V_r (km/s)	2.8	3.0	3.0	3.0	2.9	2.9

M_0 and V_r denote the seismic moment and rupture velocity, respectively

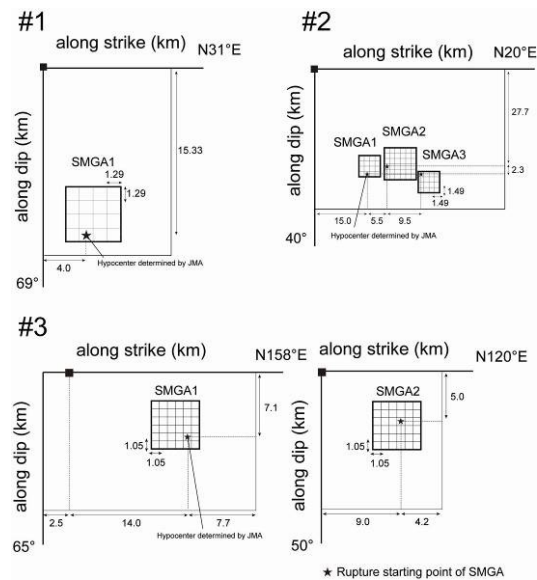


Figure 5. Source models of each earthquake. The star indicates the rupture starting point of each SMGA.

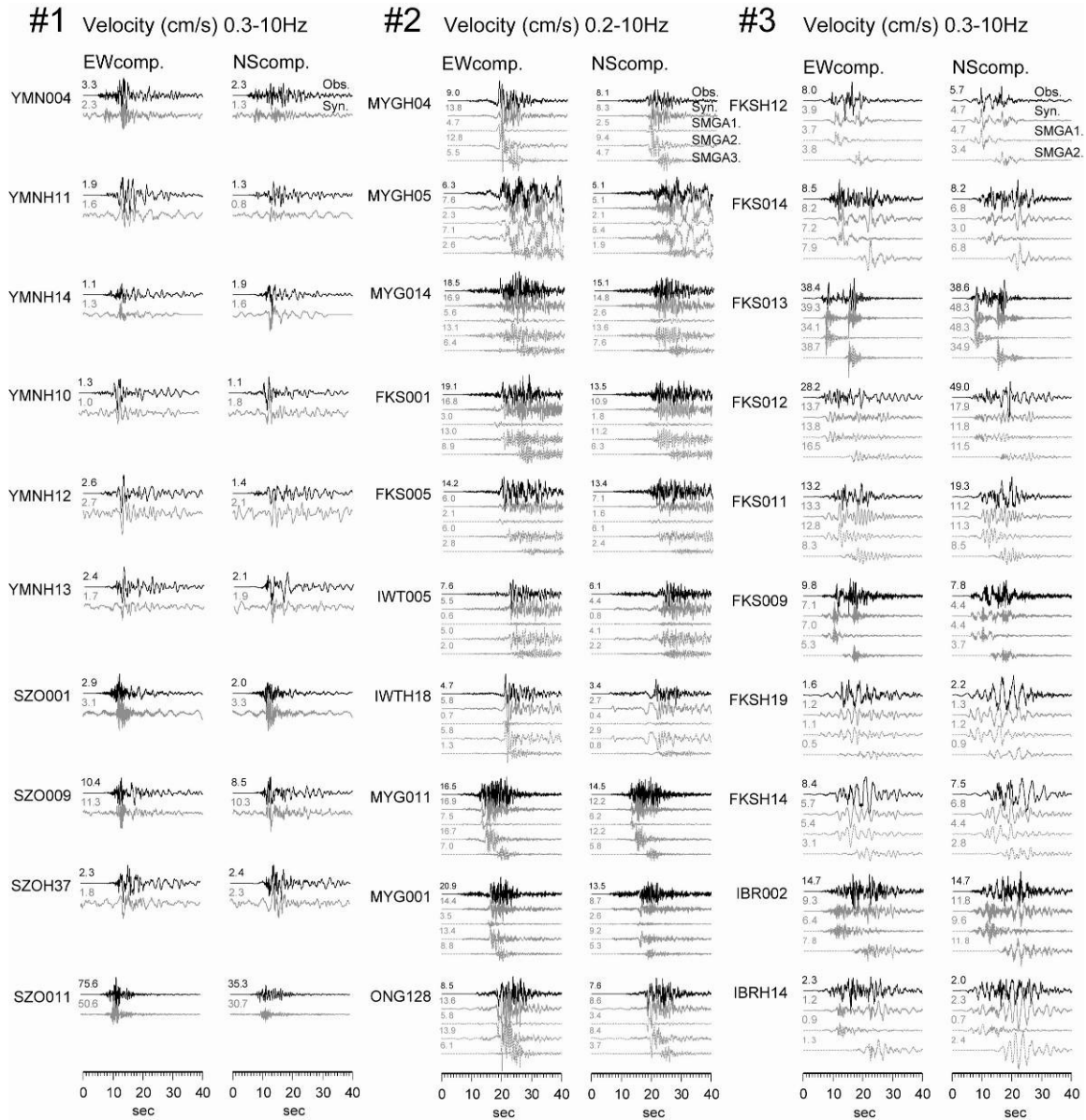


Figure 6. Examples of Comparisons among observed velocity waveforms (solid black line), synthetic waveforms (solid gray line) and synthetic waveforms generated from each SMGA (dashed gray line). The two horizontal components are shown. Number indicates the maximum amplitude of each velocity waveforms in cm/s.

4. SCALING RELATIONSHIPS

In Figure 7, we compare the relationship between the SMGA parameter and seismic moment with the results of previous studies for inland crustal earthquakes (Miyake *et al.*, 2003) and intra-slab earthquakes (Sasatani *et al.*, 2006, Iwata and Asano, 2011). For comparison, the empirical relationship of combined asperity area and seismic moment obtained by Somerville *et al.* (1999) are also shown. The SMGA sizes of inland crustal event No.1 and No.3 are plotted within the deviation range of the empirical relationship of the other earthquakes collected by Somerville *et al.*, (1999), and that of intra-slab event No.2 is nearly comparable to the empirical relationship of Iwata and Asano, (2011). Intra-slab events have clearly smaller SMGAs and asperities compared to inland crustal events having the same seismic moment. There are no differences (or variations) in the scaling relationships with the results of previous studies for three induced earthquakes caused by the great inter-plate earthquake.

In the same way, rise times of inland crustal events collected in this study are similar to the empirical relationships of previous studies. For intra-slab events including event No.2, rise times are approximately 0.3 times smaller than those of inland crustal events under the same seismic moment. To validate this tendency, we should analyze more source models in future study.

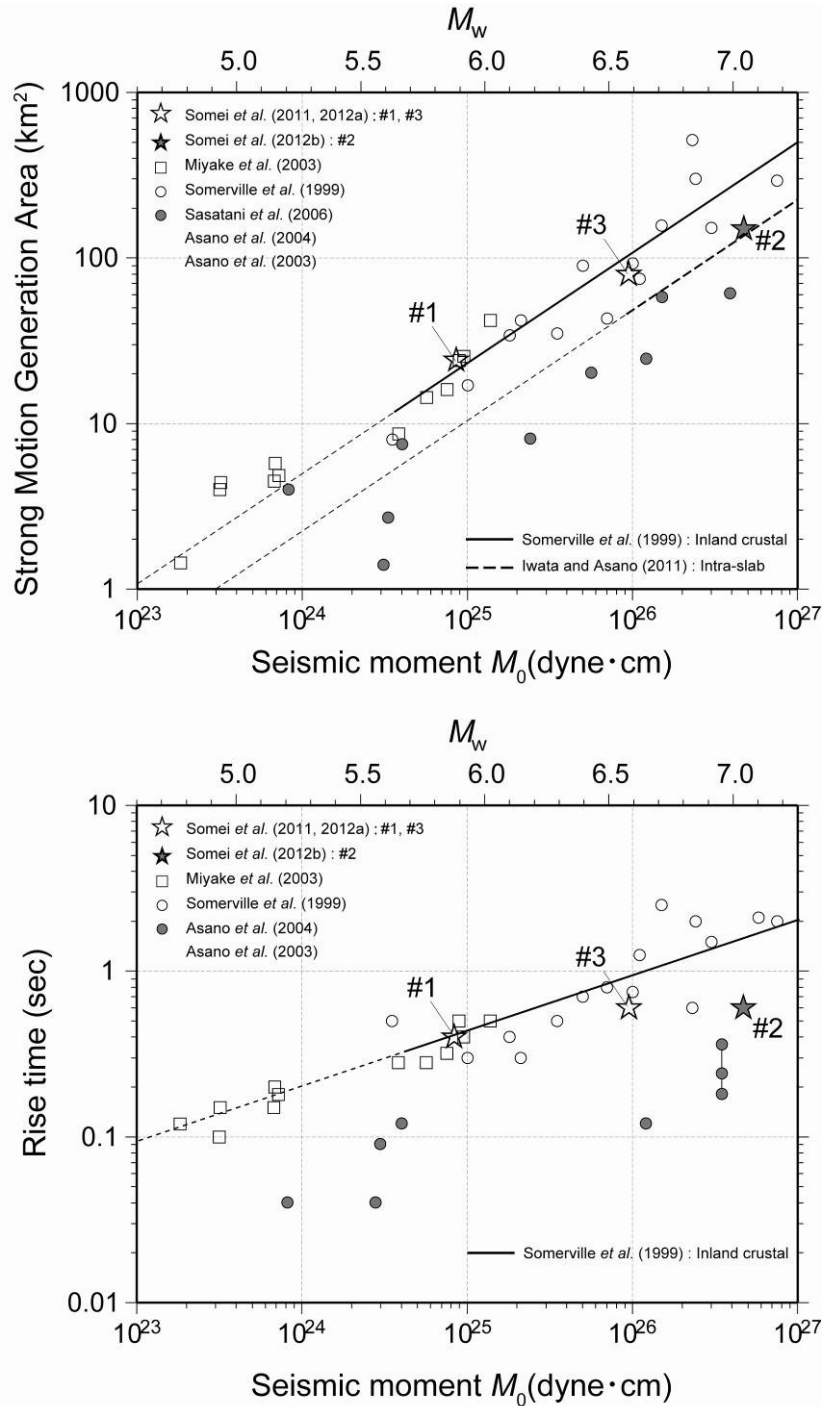


Figure 7. Top: Scaling of the strong motion generation area (SMGA) to seismic moment M_0 . Bottom: Scaling of the rise time to seismic moment M_0 . Open symbols show the parameters for inland crustal earthquakes, and solid symbols show the parameters for intra-slab earthquakes. The solid line indicates the empirical relationship of combined asperity area and M_0 for inland crustal earthquakes obtained by Somerville *et al.* (1999). The dashed line indicates the empirical relationship of SMGA and M_0 for intra-slab earthquakes obtained by Iwata and Asano (2011).

5. CONCLUSIONS

From the forward strong motion simulations, the characterized SMGA source models of three induced earthquakes caused by the 2011 Tohoku earthquake were estimated to investigate the strong motion generation process. We found that the extreme large ground motions near the source areas have been caused by the forward directivity effects during source rupture processes and by the site amplifications. On the other hand, The SMGA parameters of these events (two inland crustal events and one intra-slab event) even with the normal fault-type mechanism follow roughly the empirical scaling relationships for each tectonic environment, i.e. for inland crustal earthquakes, for intra-slab earthquake.

ACKNOWLEDGEMENTS

Strong motion records were provided from K-NET, KiK-net and F-net operated by National Research Institute for Earth Science and Disaster Prevention Japan (NIED), and Tohoku Electric Power Company (Tohoku-EPCO). The Tohoku-EPCO data were obtained from Japan Association for Earthquake Engineering (JAEE). The hypocenter information was providing by Japan Meteorological Agency (JMA) and moment tensor by F-net of NIED. We thank Dr. Petukhin Anatoly for improving the manuscript. Some figures were drawn by Generic Mapping Tools Ver.4.5.2 (Wessel and Smith, 1998).

REFERENCES

- Aoi, S., Obara, K., Hori, S., Kasahara, K. and Okada, Y. (2000). New strongmotion observation network: KiK-net. *Eos Trans. AGU*, **81**, F863.
- Asano, K., Iwata, T. and Irikura, K. (2003). Source characteristics of shallow intraslab earthquakes derived from strongmotion simulations. *Earth Planets Space*, **55**, e5–e8.
- Asano, K., Iwata, T. and Irikura, K. (2004). Characterization of source models of shallow intraslab earthquakes using strong motion data. *Proc. 13th World Conf. Earthq. Eng.*, paper no. 835.
- Asano, Y., Saito, T., Ito, Y., Shiomi, K., Hirose, H., Matsumoto, T., Aoi, S., Hori, S. and Sekiguchi, S. (2011). Spatial distribution and focal mechanisms of aftershocks of the 2011 off the Pacific coast of Tohoku Earthquake. *Earth Planets Space*, **63**, 669–673.
- Brune, J. N. (1970). Tectonic stress and the spectra of seismic shear waves from earthquakes. *J. Geophys. Res.* **75**, 4997–5009.
- Brune, J. N. (1971). Correction. *J. Geophys. Res.* **76**, 5002.
- Fukuyama, E., Ishida, M., Dreger, D. S. and Kawai, H. (1998). Automated seismic moment tensor determination by using on-line broadband seismic waveforms. *Zisin (J. Seism. Soc. Jpn.)* **51**, 149–156 (in Japanese with English abstract).
- Ishiyama, T., Sato, H., Sugito, N., Echigo, T., Ito, T., Kato, N. and Imaizumi, T. (2011), Tectonic setting of coseismic surface rupture associated with the 2011 Iwaki earthquake (M7.0). *Abstracts of Japan Geoscience Union Meeting, 2011*, MIS036-P105.
- Iwata, T. and Asano, K. (2011). Characterization of the heterogeneous source model of intraslab earthquakes toward strong ground motion prediction. *Pure Appl. Geophys.*, **168**, 117–124.
- Irikura, K. (1986). Prediction of strong acceleration motion using empirical Green's function. *Proc. 7th Japan Earthq. Eng. Symp., Tokyo*, 151–156.
- Kamae, K. and Irikura, K. (1998). Source model of the 1995 Hyogo-ken Nanbu earthquake and simulation of near-source ground motion. *Bull. Seism. Soc. Am.*, **88**, 400–412.
- Kinoshita, S. (1998). Kyoshin Net (K-NET). *Seism. Res. Lett.* **69**, 309–332.
- Koketsu, K., Yokota, Y., Nishimura, N., Yagi, Y., Miyazaki, S., Satake, K., Fujii, Y., Miyake, H., Sakai, S., Yamanaka, Y. and Okada, T. (2011). A unified source model for the 2011 Tohoku earthquake, *Earth Plant. Sci. Lett.*, **310**-3-4, 480–487.
- Kurahashi, S. and Irikura, K. (2011). Source model for generating strong ground motions during the 2011 off Pacific coast of Tohoku Earthquake. *Earth Planets Space*, **63**, 571–576.
- Miyake, H., Iwata, T. and Irikura, K. (2003). Source characterization for broadband ground-motion simulation: Kinematic heterogeneous source model and strong motion generation area. *Bull. Seism. Soc. Am.* **93**, 2531–2545.
- Okada, T., Yoshida, K., Ueki, S., Nakajima, J., Uchida, N., Matsuzawa, T., Umino, N., Hasegawa, A. and Group for the aftershock observations of the 2011 off the Pacific coast of Tohoku Earthquake (2011). Shallow inland earthquakes in NE Japan possibly triggered by the 2011 off the Pacific coast of Tohoku Earthquake.

- Earth Planets Space*, **63**, 749–754.
- Sasatani, T., Morikawa, N. and Maeda, T. (2006). Source characteristics of intraslab earthquakes. *Geophys. Bull. Hokkaido Univ.* **69**, 123-134 (in Japanese with English abstract).
- Si, H. and Midorikawa, S. (1999). New attenuation relationships for peak ground acceleration and velocity considering effects of fault type and site condition. *J. Struct. Constr. Eng. AIJ*, **523**, 63–70 (in Japanese with English abstract).
- Somei, K., Miyakoshi, K. and Irikura, K. (2011). Estimation of source model and strong motion simulation for the 2011 east Fukushima prefecture earthquake using the empirical Green's function method. *Abstracts of Seismological Society of Japan Meeting 2011*, P2-29 (in Japanese).
- Somei, K., Miyakoshi, K. and Kamae, K. (2012a). Source model of the 2011 East Shizuoka prefecture, Japan, earthquake by using the empirical Green's function method. *Abstracts of Japan Geoscience Union Meeting 2012*, S-SS26.
- Somei, K., Miyakoshi, K. and Okazaki, A. (2012b). Source model of the 2011 off Miyagi prefecture, Japan, intra-slab earthquake estimated by using empirical Green's function method. *Abstracts of Architectural Institute of Japan Meeting 2012*, inpress (in Japanese).
- Somerville, P., Irikura, K., Graves, R., Sawada, S., Wald, D., Abrahamson, N., Iwasaki, Y., Kagawa, T., Smith, N. and Kowada, A. (1999). Characterizing crustal earthquake slip models for the prediction of strong ground motion. *Seism. Res. Lett.* **70**, 59–80.
- Suzuki, W. and Iwata, T. (2005). Source characteristics of interplate earthquakes in northeast Japan inferred from the analysis of broadband strong-motion records. *Eos Trans. AGU*, **86**(52), S43A-1040.
- Suzuki, W. and Iwata, T. (2006). Source model of the 2005 west off Fukuoka prefecture earthquake estimated from the empirical Green's function simulation of broadband strong motions. *Earth Planets Space*, **58**, 99–104.
- Toda, S., Stein, R. S. and Lin, J. (2011). Widespread seismicity excitation throughout central Japan following the 2011 M=9.0 Tohoku earthquake and its interpretation by Coulomb stress transfer, *Geophys. Res. Lett.*, **38**, L00G03, doi:10.1029/2011GL047834.
- Wessel, P. and Smith, W. H. F. (1998). New improved version of the Generic Mapping Tools released. *Eos Trans. AGU*. **79**, 579.
- Yoshida, K., Miyakoshi, K. and Irikura, K. (2011). Source process of the 2011 off the Pacific coast of Tohoku Earthquake inferred from waveform inversion with long-period strong-motion records. *Earth Planets Space*, **63**, 577–582.